ACTA METALLURGICA SLOVACA
2021, VOL. 27, NO. 3, 146-151

RESEARCH PAPER

CHARACTERISTICS OF AISI 420 STAINLESS STEEL MODIFIED BY COMBINING GAS NITRIDING AND CrN COATING

Thanh Van Nguyen[1)], Van Thanh Doan[2)], Trung Van Trinh[1)], Huy Van Vu[2)]*

[1)] Hanoi University of Science and Technology, Hanoi, Vietnam, No.1 Dai Co Viet Street, Hai Ba Trung District, Hanoi city, Vietnam

[2)] Southern Branch, Vietnam-Russian Tropical Centre, No. 3, 3/2 Street, 11Ward, 10 District, Ho Chi Minh city, Viet Nam

* Corresponding author: trung.trinhvan@hust.edu.vn, Tel.: +84 24 3868 0409, School of Materials Science and Engineering, Hanoi University of Science and Technology, 11657, No.1 Dai Co Viet Street, Hai Ba Trung District, Hanoi city, Vietnam

Received: 07.07.2021
Accepted: 26.08.2021

ABSTRACT

AISI 420 stainless steel is widely used in applications where good mechanical properties and corrosion resistance are required. However, the heat treatment and nitriding process can reduce the corrosion resistance of this stainless steel. This article focuses on investigating the influence of tempered substrate and efficiency of the gas nitriding at temperatures of 520 °C and 550 °C on some properties of CrN coating. The experiments were carried out to evaluate the surface hardness, microstructure and phase composition of nitrided layers. The coating adhesion and load capacity of the coating were performed according to VDI 3198 standard. Electrochemical testing was performed in a solution of 3.5% NaCl and then using the Tafel method to determine the corrosion current and corrosion potential. The thickness of CrN and CrN/CrN coating was 1.6 µm and 3 µm, respectively. The study showed that the corrosion resistance of coatings fabricated through duplex technology was affected not only by the normal defects but also by the porosity on the nitrided surface. The multilayer duplex coating improved a better corrosion resistance than mono-layer duplex coating due to its ability to cover and reduce pores and pitting defects.

Keywords: Arc-PVD; martensitic stainless steel; gas nitriding; CrN coating; corrosion-resistant; duplex coating

INTRODUCTION

Stainless steel plays an increasingly important role in industries due to its corrosion resistance, hygienic properties, aesthetic appeal, etc. Currently, stainless steel is being studied in diverse directions like metallurgy [1-4], heat treatment [5-10], thermo-chemical treatment [11-18] and coating technologies [19, 20]. Martensitic stainless steels like 410, 420, 440A grade are widely used as moulds for plastic injection and glass moulding, cutting tools, structural parts, automotive components, surgical and dental instruments, where high strength, wear and corrosion resistance are required [11, 12].

Bjarbo and Hatterstrand [5] reported that for the steel grade with content of carbon higher than 0.2% and Cr 12-13%, the annealed steel included the carbides M_3C, M_7C_3 and $M_{23}C_6$ (where M is alloy element). The mechanical properties and corrosion resistance depend on the solubility of these carbides into matrix during austenitization and on carbide precipitation during tempering [5, 7]. Austenitization temperature of this steel grade at 1000÷1040 °C gave an optimum percentage of carbide distribution in the matrix which resulted in increasing the hardness and corrosion resistance [8, 12]. For application required only heat treatment, tempering temperature should be chosen below 370 °C to ensure the corrosion resistance [9].

Kerl-Erick Thelning [21] recommended that martensite stailess steel should be nitrided in the temperature interval from 520 °C to 550 °C, while austenite stailness steel should be nitrided from 570 °C to 620 °C. On the other hand, at this temperature nitriding process generates the chrome nitride CrN and the chromium content was decreased as result, thus corrrosion resistance was also decreased. Pilch et al.[22] performed plasma nitriding at 515 °C and 525 °C for turbocharger stator made of X12Cr13 steel and found that corrosion reistance of untreated surface was better than nitrided one. Other studies also confirmed this phenomenon [14, 23].

Many studies tried to conduct nitriding in plasma at a lower temperature (below 500 °C) to improve the corrosion and wear resistance of carbon and low alloy steels [13, 24, 25]. Unfortunately, the effect of this technique is very limited for cold working steels and martensite stainless steel due to the low productivity [23]. Yang Li et al. [26] performed Active screen plasma nitring for AISI 420 steel at 440 °C and 480 °C for 6 hours, the corrosion resistance was improved but the nitrided layer was too thin (18 µm and 25 µm). Salt bath nitriding (SBN) can form nitrided layer at very low temperature (400 °C). Funatani reported the SBN at 480 °C dies for hot deformation and extrusion [27]. For stainless steels SBN is usually performed at temperature above 520 °C due to melting temperature, fluidity of melted salts and passive layer of chrome oxide. Unlike the SBN, gas-nitriding temperature was recommended at 495 °C ÷ 570 °C [28]. Kolsterising, a carburizing process, is an effective method to treat stainless steel. This technology can produce at 450 °C but it requires a long treatment time (up to 24 hours) [29]. Otherwise, this technology is still not widely spread over the world.

Duplex technology characterized by combining nitriding and coating is a very natural idea to promote hardness, corrosion resistance, wear resistance and high temperature resistance of nitrided layer. The coating can be deposited by various methods, such as electroplating, chemical immersing, chemical vapour deposition (CVD), physical vapour deposition (PVD),

etc. [20, 23, 32]. Other studies presented duplex layer-coating technology on the AISI 420 steel [30, 31].
From viewpoint of technology investment, gas nitriding is still popular modified surface technology, in particular in developing countries. An important note is that for the martensite stainless steel, the gas nitriding forms a thick compound layer with high porosity. The pores appear not only in the outermost layer of the surface, where there are many nitrogen-rich phases like $Fe_{2\text{-}3}N$ or Fe_4N but they can be also generated in the diffusion layer because unstable α-Fe(N) phase decomposes into α-Fe(N)* and nitrogen gas [33, 34]. The growth of nitrogen gas leads to growth of pores in the diffusion layer [16]. The number of pores in nitrided layer for gas nitriding was higher than for plasma nitriding due to the low energy of the N atoms, they tend to recombine to form nitrogen gas [34].
AISI 420 martensite stainless steel is a meaningful grade in manufacturing PET (PolyEthylene Terephthalate) die mould [31]. Cause of the operation conditions, the heat treatment is not enough to improve the wear of the die mould. There are not many studies on duplex coating combined gas nitriding and coating on this steel yet. In addition, the effect of surface morphology on duplex coating quality was not much detailed. Therefore, this study focuses on investigating the influence of nitrided layer structure (compound layer thickness) and surface morphology (porosity) on the adhesion and corrosion behaviour of duplex coating fabricated through gas nitriding and CrN coating on the AISI 420 steel.

MATERIALS AND METHODS

Material and surface modification

The samples in the dimension of 12 mm diameter x 7 mm thickness were made from AISI 420 martensitic stainless steel. The chemical composition of steel was verified using Optical Emission Spectrometry ARL3460. The measured results are listed in **Table 1**.

Table 1 Chemical composition of experimental steel (wt.%)

	C	Mn	Si	Cr	Ni	V	Mo	P	S
AISI 420	0.15-0.4	≤1	≤1	12.0-14.0	-	-	-	≤0.04	≤0.03
Measured	0.379	0.427	0.833	13.49	0.177	0.219	0.100	0.018	0.001

These samples were austenitized in the vacuum furnace at 1030 °C for 1.5 hours, following quenched in nitrogen gas with the gas pressure of 1.5 bar. With this pressure, the cooling rate was about 20 °C/min, the hardness after quenching was 55÷56 HRC. After that, the samples were tempered at 580 °C for 4 hours. The hardness after tempering was 42 HRC. Before gas nitriding, the samples were sequentially ground by abrasive papers with grit size to 2000, then sandblasted to remove the chromium oxide layer.
The nitriding atmosphere consisted of ammonia and nitrogen gas with a decomposition ratio of about 24% (nitriding potential K_N = 7.2). The gas nitriding process was carried out in two variants of temperature: 520 °C (LN - Low-Temperature Nitriding) and 550 °C (HN - High-Temperature Nitriding) for 5 hours. All tempered and nitrided samples were ground with sandpaper #1200, #1500, and then polished using 3 µm Cr_2O_3 abrasive suspension. The sample was fixed on a holder which enable to keep in hand to grind. A micrometer with accuracy of 1 µm was used to control the thickness of the sample to remove by grinding and polishing process. The aim of this step is to the oxide layer on the surface which affects the properties of the duplex coating [35] and improve surface roughness after nitriding procees to attain surface of pre-coated sample to have the unique surface roughness.
The sample surface was cleaned in alcohol using the ultrasonic bath. Intermediate Cr coating and CrN coating were conducted on nitrided surfaces using Dreava-400 coating system with the following process parameters: Cr target with a purity of 99.99 %, temperature of 300 °C, vacuum pressure of 2.4×10^{-2} Pa, argon gas flow of 20 mL/min, the arc current of 60 A. The bias voltage -40 V was applied to reduce the creation of macroparticles on the surface. The Cr coating was deposited for 60 seconds, then nitrogen gas was added to the chamber with a flow rate of 200 mL/min to form a CrN compound film. The mono-layer coating CrN was deposited for 30 minutes. The symbols H/CrN, LN/CrN and HN/CrN were used to refer mono-layer coating on the tempered, low temperature (520 °C) and high temperature (550 °C) nitrided substrates. The multi-layer CrN/CrN coating was performed on mono-layer CrN coating. Before second deposition, the samples were polished again to remove macroparticles, subsequently repeated procedure as the first deposition. Thus, this sample group had a total deposition duration of 60 minutes.
The experimental samples were marked as shown in **Table 2**.

Table 2 Marking experimental samples

Identification	Meaning
H	Heat treatment (quenching + tempering)
LN	Gas nitriding at temperature 520°C
HN	Gas nitriding at temperature 550°C
H/CrN	Heat treatment + CrN coating
LN/CrN	Gas nitriding 520°C + Cr coating + CrN coating
HN/CrN	Gas nitriding 550°C + Cr coating + CrN coating
LN/CrN/CrN	Gas nitriding 520°C + Cr coating + CrN coating + polished + Cr coating + CrN coating
HN/CrN/CrN	Gas nitriding 550°C + Cr coating + CrN coating + polished + Cr coating + CrN coating

Characterizations of the modified surface

The surface roughness of samples was measured using a Keyence VHX-700 stereomicroscope. The layer/coating structure was captured and analyzed using Axiovert 40 MAT optical microscope, JSM-7600 scanning electron microscope accompanied with Xmax 50 EDS probe and Panalytical X'Pert Pro X-ray diffractometer.
The Marble etching solution (4 g $CuSO_4$: 25 ml HCl : 25 HNO_3) was used to observe the nitrided substrate structure of cross-section samples. The surface hardness HV0.1 were measured using Future - Tech Corp 700 hardness tester. The adhesion of the coatings to the substrates was studied using an HRC indentor with a load of 150 kg.f, then the imprints were captured by microscope and evaluate obtained images according to VDI 3198 standard (the principle illustrated in **Fig. 1**). In addition, the diameter and depth of the HRC imprint were also measured.

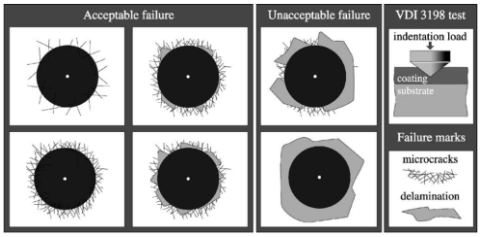

Fig. 1 Principle of indentation assessment according to VDI 3198 standard [36]

An electrochemical test was performed on the Autolab PGSTAT302N device using a standard three-electrode cell with a platinum counter electrode and a saturated calomel

electrode as the reference electrode. The used electrolyte, 3.5 % NaCl solution, was reduced oxygen by plunging nitrogen for 1 hour. Before scanning, the sample was installed in the electrode cell and immersed 30 minutes in the electrolyte, the contact square of the sample was 1 cm^2. The test was performed with a scan rate of 1 mV/s. After each potentiodynamic polarization test, the corrosion potential (E_{corr}) and the corrosion current density (i_{corr}) were determined from the Tafel plot.

RESULTS AND DISCUSSION

Surface hardness and microstructure

Measured surface hardness is presented in **Fig. 2**. There are three groups of columns: The first group refers to substrate before coating (H-tempered, LN-Low temperature nitriding, HN-High temperature nitriding), the second one refers to mono-layer coating substrate/CrN and the last one refers to multilayer coating substrate/CrN/CrN. Each group is ordered by tempered, LN and HN samples.

In general, the hardness of tempered substrate was considerably improved by nitriding: The hardness of tempered sample was just 450 HV0.1, the LN and HN nitrided samples were 1162 HV0.1 and 1241 HV0.1 respectively. The high-temperature nitriding showed a greater hardness than the low-temperature nitriding; the multilayer coatings have a greater hardness than the mono-layer coating in the same type (CrN or CrN/CrN): After multilayer coating CrN/CrN, the hardness of H/CrN/CrN, LN/CrN/CrN and HN/CrN/CrN samples were 1150, 1521 and 1787, while after mono-layer coating the hardness of H/CrN, LN/CrN and HN/CrN samples reached the values of 1010, 1450 and 1639 HV0.1. Because the coatings were thin, the difference hardness of coatings is tightly related to the hardness of the substrate.

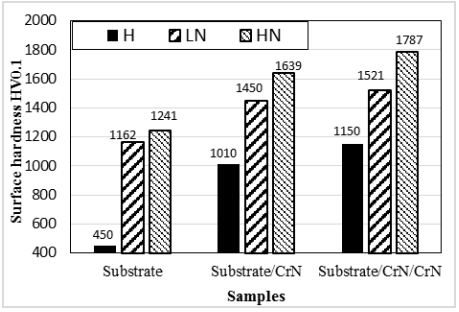

Fig. 2 Surface hardness of samples

The roughness parameter Ra of H, LN and HN substrates before coating were 0.13 µm, 0.28 µm and 0.33 µm respectively. The case depth of the nitrided substrate LN and HN before coating was 48 ±1 µm and 50 ±1 µm, respectively. Compared with the original nitrided sample, the compound layer of the LN and HN samples was removed by roughly 2 µm and 5 µm by grinding and polishing.

The LN nitrided layer consists of the compound layer and the diffusion layer, while the HN consists of only one layer so-called "nitrided layer". The case depth of the LN and HN samples was about 50 ±1 µm and 55 ±2 µm, respectively. The LN sample had a compound layer about 19 ±1 µm thick. On the cross-section of the nitrided sample, cracks can be observed at the thick compound layer. The Ra parameter of the HN and LN samples was 4.56 µm and 1.96 µm, respectively.

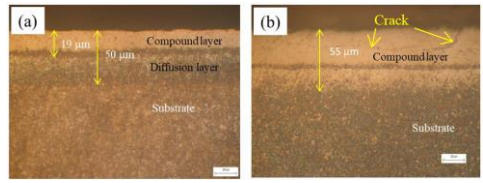

Fig. 3 Nitrided layers of samples (a) Low-temperature nitriding LN; (b) High-temperature nitriding HN

The cross-section structure of the coating on the nitrided substrate is shown in **Fig. 4**. After grinding and polishing, the case depth of HN sample was 50 µm. Measured results on SEM image showed that the coating thickness of mono-layer coating CrN was about 1.6 µm, the multilayer coating CrN/CrN was about 3 µm. The cracks that appeared on the HN substrate was generated at some locations of the compound layer, where the pores existed.

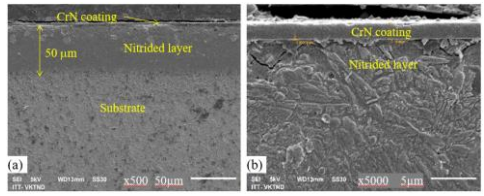

Fig. 4 Microstructure of HN/CrN sample
a) SEM 500x b) SEM 5.000x

Porosity

As reported in [13], the nitrided layer of AISI 420 martensitic stainless steel consisted of a thick compound layer consisting of ε-$Fe_{2-3}N$, γ'-Fe_4N phases at both temperatures 480 °C and 560 °C. The uniform compound layer with small porosity exhibited better corrosion resistance than the compound layer with higher porosity. The phase composition of nitrided samples (LN and HN samples) measured by the X-ray diffraction technique is shown in **Fig. 5**. The ε- $Fe_{2-3}N$ and γ'-Fe_4N phases were found. In addition, the Fe_2O_3 phase also existed on the HN/CrN sample, possibly due to the high porosity, therefore oxygen has penetrated the nitrided layer to create iron oxide.

Porosity appeared on and within the outermost layer of the surface, where there are many rich-nitrogen $Fe_{2-3}N$, Fe_4N phases. The porosity was calculated from 5 pictures captured at various postions on the surface. When increasing the nitriding temperature from 520 °C to 550 °C (HN sample), the porosity on surface after grinding and polishing increased from 5% (**Fig. 6a**) to 15% (**Fig. 6b**). The different in porosity can be refer to the amount of ε-$Fe_{2-3}N$ phase: With the increase of temperature, the amount of ε-$Fe_{2-3}N$ phase in the nitrided surface increases, while the amount of α-N and γ'-Fe_4N phases decreases significantly [16]. It leads to the higher porosity after high-temperature nitriding.

On the surface of the LN/CrN, it can be found macroparticles. On the surface of the HN/CrN sample (**Fig. 6d**), there are macroparticles and pore defects. These defects can be the deepest pore location of the nitrided layer that coating could not completely cover.

Adhesion and load resistance

The test adhesion results of coating on various substrates determined according to the VDI 3198 standard are shown in **Table 3** and **Fig. 7**.

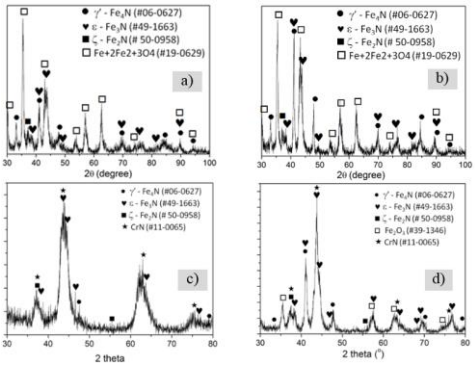

Fig. 5 Phase analysis XRD of nitrided and mono-layer coating CrN samples a) LN; b) HN; c) LN/CrN; d) HN/CrN

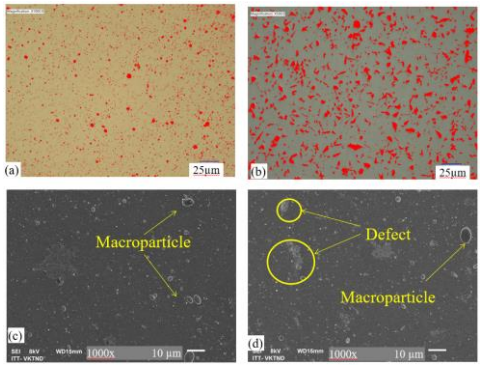

Fig. 6 Porosity analysis of nitrided surface **(**the red colour indicated pores) a) LN b) HN c) LN/CrN d) HN/CrN

Table 3 Summary of adhesion assessment of coatings

Sample	HRC imprint depth (µm)	HRC imprint diameter (µm)	Adhesion
H/CrN	165	748	HF6
LN/CrN	127	563	HF3
LN/CrN/CrN	135	560	HF3
HN/CrN	125	540	HF2
HN/CrN/CrN	120	555	HF2-HF3

The imprint on the H/CrN sample (**Fig. 7a**) did not form the radial cracks, therefore the adhesion between the substrate and the coating can be classified as HF6. For the LN/CrN and HN/CrN samples, several radial cracks and peeling around the imprint can be observed with different levels. The number of radial cracks of imprint in the case of the HN/CrN surface (9 lines) is less than the number of lines on the LN/CrN surface (14 lines). According to VDI 3198 standard, the adhesion of the HN/CrN sample was HF2, LN/CrN sample was HF3. However, on the imprint circµmference of the HN/CrN sample, there was more coating peeling than on the LN/CrN sample cause of the harder but more brittle HN layer. The multilayer coatings LN/CrN/CrN sample had the adhesion value of HF3 and HN/CrN/CrN sample between HF2-HF3.

The diameter and depth of imprint are useful to estimate adhesion and load capacity of substrate – coating system [37]. The mono-layer coating on tempered substrate showed the largest depth (165 µm) and diameter (748 µm), due to the low hardness (450 HV0.1), the hardness difference between the coating and the substrate is the highest. The nitrided substrates had a better load capacity of substrate – coating system: The imprint depth was only about 125 ÷ 127 µm, the diameter of the LN/CrN was 571 µm compared to 540 µm for the HN/CrN sample. The reason can be explained by the high hardness of the HN/CrN sample (1639 HV0.1), which supports the load capacity better than the LN/CrN sample with low surface hardness (1450 HV0.1). In addition, the porosity of the nitrided HN sample was greater than the nitrided LN sample, which can also be caused by the increased adhesion of the coating to the substrate.

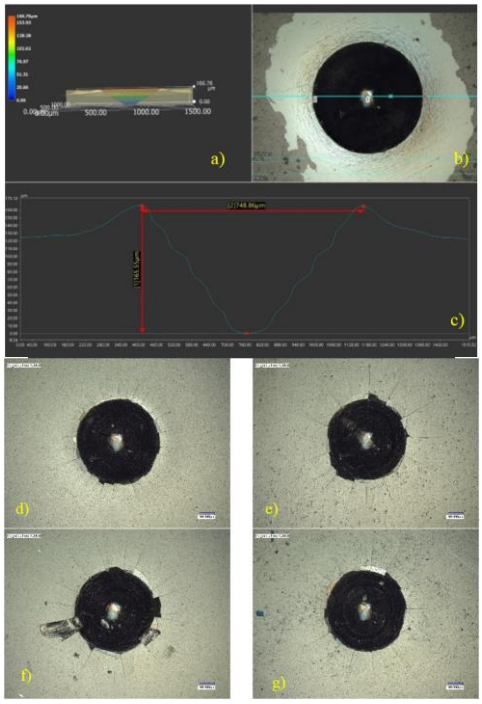

Fig. 7 Imprint images of adhesion test (a) 3D view of the imprint; (b) H/CrN; (c) measurement of the imprint diameter; (d) LN/CrN; (e) HN/CrN; (f) LN/CrN/CrN; (g) HN/CrN/CrN

Corrosion behavior

The polarization curves of electrochemical measurements are shown in **Fig. 8**. The corrosion potential E_{corr} and corrosion current i_{corr} was determined by extrapolation of Tafel curves as shown in **Fig. 9**.

The results confirmed the decrease of corrosion resistance of both nitrided LN and HN samples compare to tempered sample as results of chromium concentration decrease in steel and pore formation in the compound layer, as mentioned in [7, 8, 13].

In addition, the low-temperature nitriding LN showed a better corrosion behaviour than the high-temperature nitriding HN due to lower i_{corr} (4.75 mA/m^2 vs. 8.07 mA/m^2) and more positive E_{corr} (-0.46 V vs. -0.508 V). This effect is related to the

porosity of nitrided substrate detailed above. Likewise, with the same CrN coating process, the LN/CrN and LN/CrN/CrN samples exhibited better corrosion results than HN/CrN and HN/CrN/CrN samples. The pores existed on nitrided surface were covered by CrN coating, but at the defect locations due to holes and pinholes, corrosive agents penetrated deeply into the substrate through the pores to the compound layer, even to the diffusion layer.

By impressively reducing corrosion current density i_{corr} simultaneously increasing corrosion potential E_{corr}, the CrN coating exhibited a good ability to improve the corrosion resistance of substrate, not only nitrided samples but also tempered samples. This effect observed on multilayer coating CrN/CrN was better on mono-layer coating CrN due to greater thickness and polished surface before the second deposition.

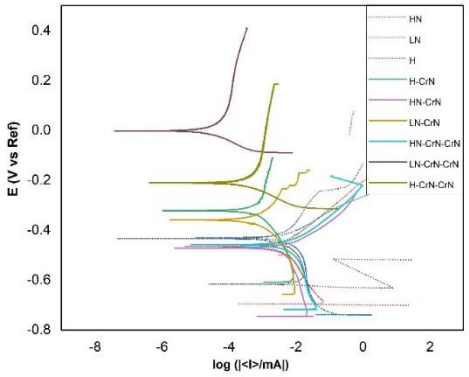

Fig. 8 Electrochemical polarization curves of samples

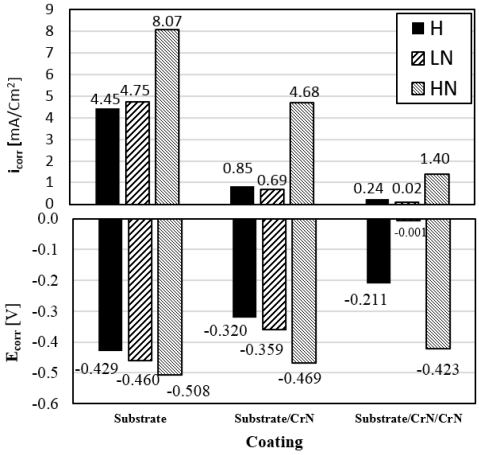

Fig. 9 Results of Tafel determination of corrosion current density and corrosion potential difference

CONCLUSION

This study presents the formation of a nitrided layer on the tempered substrate, the deposition of mono-layer CrN and multilayer CrN/CrN on the nitrided substrate, the influence of nitrided layer structure (compound layer thickness) and surface morphology (porosity) on the adhesion and corrosion resistance of duplex coating fabricated by gas nitriding and cathode arc deposition.

Gas nitriding at 520 °C formed the nitrided layer with a similar case depth to nitriding at 550 °C (50 µm vs. 55 µm). The XRD analysis results showed more rich-nitrogen ε-Fe_2-3N and γ'-Fe_4N phases found on the nitrided surface 550 °C. The amount of epsilon phase explains why the hardness of the HN sample was greater and also more porosity than the LN sample.

For the mono-layer coating CrN, the coating-nitrided substrate system improved the adhesion and load capacity compared with the coating-tempered system. In the corrosion test, the cover effect of the CrN coating on tempered and LN substrates was good enough, so the icorr value was decreased from 5 to 7 times. Due to the more porosity of nitrided layer LN, the LN/CrN sample had a slightly decreased icorr value from 8.07 mA/m2 to 4.68 mA/m^2.

For the multilayer coating CrN/CrN, the adhesion and load capacity of the coating-substrate system was similar to the mono-layer coating. The mechanical polishing, intermediate coating Cr even function coating CrN allowed to fill in pores resulted in reducing the defect on the surface substrate and therefore increased corrosion resistance impressively. The icorr value decreased 18.5, 237.5 and 5.8 times compared to corresponded tempered, LN nitriding and HN nitriding substrate.

ACKNOWLEDGEMENTS

This research is supported by the Hanoi University of Science and Technology under the project number T2020-SAHEP-040.

REFERENCES

1. T. Kvackaj, J. Bidulská, R. Bidulský: Materials, 14(8), 2021, 1988. https://doi.org/10.3390/ma14081988.
2. R. Bidulsky, J. Bidulská, F. S. Gobber et al.: Materials, 13(15), 2020, 3328. https://doi.org/10.3390/ma13153328.
3. P. Petrousek, T. Kvackaj, R. Kocisko, J. Bidulska, M. Luptak, D. Manfredi, M.A. Grande, R. Bidulsky: Acta Metallurgica Slovaca, 25(4), 2019, 283-290. https://doi.org/10.12776/ams.v25i4.1366.
4. R. Bidulsky, M.A. Grande, E. Dudrova, M. Kabatova, J. Bidulska: Powder Metallurgy, 59(2), 2016, 121-127. https://doi.org/10.1179/1743290115Y.0000000022.
5. A. Bjarbo, M. Hattestrand: Matallurgical and Materials Transactions A, 32, 2001, 19-27. https://doi.org/10.1007/s11661-001-0247-y.
6. M.G. Minciuna, D.C. Achitei, P. Vizureanu, A.V. Sandu, M. Nabialek: Acta Physica Polonica A, 135, 2019, 115-118. http://doi.org/ 10.12693/APhysPolA.135.115.
7. A. C. Iftikhar, H. A. Shahid, A. S. Aqeel, D. C. Ali: Sukkur IBA University Journal of Emerging Technologies, 2(1), 2019, 51-56. https://doi.org/10.30537/sjet.v2i1.
8. V. A. Kumar, M. K. Karthikeyan: Materials Science Forum, 710, 2012, 489-494. https://doi.org/10.4028/www.scientific.net/msf.710.489.
9. M. S. Anwar, S. Prifiharni, E. Mabruri: The effect of tempering temperature on pitting corrosion resistance of 420 stainless steels. In: *The 3rd International Conference on Advanced Materials Science and Technology (ICAMST 2015), AIP Conf. Proc.* 1725(1), 020005-1–020005-8. http://doi.org/10.1063/1.4945459.
10. Yr. Liu, D. Ye, Ql. Yong, J. Su, Ky. Zhao, W. Jiang: Journal of Iron and Steel Research, International, 18(11), 2011, 60-66. https://doi.org/10.1016/S1006-706X(11)60118-0.
11. C. E. Pinedo, W. A. Monteiro: Surface and Coatings Technology, 179(2-3), 2004, 119-123. https://doi.org/10.1016/S0257-8972(03)00853-3
12. A.N. Isfahany, H. Saghafian, G. Borhani: Journal of Alloys and Compounds, 509, 9, 2011, 3931-3936. https://doi.org/10.1016/j.jallcom.2010.12.174.

13. C.X. Li, T. Bell: Corrosion Science, 48(8), 2006, 2036-2049. https://doi.org/10.1016/j.corsci.2005.08.011.
14. Y. T. Xi, D. X. Liu, D. Han: Surface and Coatings Technology, 202(12), 2008, 2577-2583. https://doi.org/10.1016/j.surfcoat.2007.09.036.
15. W. Ye, X. Tong: Advanced materials research, 1004-1005, 2014, 743-746. https://doi.org/10.4028/www.scientific.net/AMR.1004-1005.743.
16. Y. Li, Y. He, J. Xiu, W. Wang, Y. Zhu, B. Hu: Surface & Coatings Technology, 329, 2017, 184-192. https://doi.org/10.1016/j.surfcoat.2017.09.021.
17. D. H. Mesa, A. Toro, A. Sinatora, A. P. Tschiptschin: Wear, 255, 2003, 139-145. https://doi.org/10.1016/S0043-1648(03)00096-6.
18. P. R. Cardoso, J. C. Scheuer, F. S. Brunatto: Corrosion resistance of plasma nitride AISI 420 martensitic stainless steel: Influence of the pretreatment and treatment temperature. In: *69th ABM International Annual Congress and to the ENEMET*, 2014, 7995-8005. https://doi.org/10.5151/1516-392X-24785.
19. T. Aizawa, T. Yoshino, K. Morikawa, S. Yoshihara: Crystals, 9(60), 2019, 1-10. https://doi.org/10.3390/cryst9020060.
20. T. Michler, M. Grischke, K. Bewilogua, H. Dimigen: Thin Solid Films, 322(1-2), 1998, 206-212. https://doi.org/10.1016/S0040-6090(97)00959-0.
21. K. E. Thelning: *Steel and its heat treatment*, 2nd ed., Butterworth-Heinemann, ISBN 9781-48316-342-0, 2013.
22. O. Pilch, P. Faltejsek, V. Hrubý, M. Krbata: Manufacturing Technology, 17(3), 2017, 360-364. https://doi.org/10.21062/ujep/x.2017/a/1213-2489/MT/17/3/360.
23. C. Ruset, E. Grigore, T. Glaser, S. Bausch: Journal of optoelectronics and advanced materials, 9(6), 2007, 1637-1644.
24. M. Krbaťa, J. Majerík, I. Barényi, I. Mikušová, D. Kusmič: Manufacturing Technology, 19(2), 2019, 238-242. https://doi.org/10.21062/ujep/276.2019/a/1213-2489/mt/19/2/238.
25. D. Kusmic, D.T. Van, V. Hruby: Manufacturing Technology, 18(2), 2018, 259-265. https://diorg/10.21062/ujep/88.2018/a/1213-2489/MT/18/2/259.
26. Y. Li, Y. He, J. Xiu, W. Wang, Y. Zhu, B. Hu: Surface and Coatings Technology, 329, 2017, 184–192. https://doi.org/10.1016/j.surfcoat.2017.09.02.
27. K. Funatani: Metal Science and Heat Treatment, 46(7), 2004, 277-281. https://doi.org/10.1023/B:MSAT.0000048834.48163.2e.
28. ASM Handbook: *Volume 04, Steel Heat Treating*, ASM International, ISBN 9780-87170-379-8, 1991.
29. D. Kovács, J. Dobránszky: Periodica Polytechnica Mechanical Engineering, 63(3), 2019, 214–219. https://doi.org/10.3311/PPme.13921.
30. K. Yamane, N. Kawagoishi, Y. Maeda, K. Morino, F. Nishimura, M. Oki: Journal of the society of materials science Japan, 59(7), 2010, 521-526. http://doi.org/10.2472/jsms.59.521.
31. E. L. Dalibon, A. Cabo, J. Halabi, R. D. Moreira, K. Silva, S. P. Bruhl: Key Engineering Materials, 813, 2019, 135-140. https://doi.org/10.4028/www.scientific.net/KEM.813.135.
32. T. Morita, K. Andatsu, S. Hirota, T. Kumakiri, M. Ikenaga, C. Kagaya, Materials Transactions, 54(5), 2013, 732-737. https://doi.org/10.2320/matertrans.M2012426.
33. B. Schwarz, H. Gohring, S.R. Meka, R.E. Schacherl, E. J. Mittemeijer: Metallurgical and Materials Transactions A, 45A, 2014, 6173-6186. https://doi.org/10.1007/s11661-014-2581-x.
34. M. Pellizzari, A. Molinari, G. Straffelini: Materials Science & Engineering: A, 352(1-2), 2003, 186-194. https://doi.org/10.1016/S0921-5093(02)00867-5.
35. J. Vega, H. Scheerer, G. Andersohn, M. Oechsner: Corrosion Science, 133(4), 2018, 240-250. https://doi.org/10.1016/j.corsci.2018.01.010.
36. *Verein Deutscher Ingenieure Normen*, VDI 3198, VDI-Verlag, Dusseldorf, 1991.
37. C. Tan, K. Zhou, T. Kuang, Y. Li, W. Ma: Surface Engineering, 34(7), 2018, 520-526. https://doi.org/10.1080/02670844.2017.1370881.